ELSEVIER

Thermochimica Acta 324 (1998) 77–85

thermochimica acta

Melting by temperature-modulated calorimetry[1]

Bernhard Wunderlich[a,*], Iwao Okazaki[2,a], Kazuhiko Ishikiriyama[3,b], Andreas Boller[b]

[a] *Depart. of Chemistry, The University of Tennessee, Knoxville, TN 37996-1600, USA*
[b] *Chem. and Anal. Sci. Div., Oak Ridge Natl. Lab., Oak Ridge, TN 37831-6197, USA*

Abstract

Well-crystallized macromolecules melt irreversibly due to the need of molecular nucleation, while small molecules melt reversibly as long as crystal nuclei are present to assist crystallization. Furthermore, imperfect crystals of low-molar-mass polymers may have a sufficiently small region of metastability between crystallization and melting to show a reversing heat-flow component due to melting of poor crystals followed by crystallization of imperfect crystals which have insufficient time to perfect before the modulation switches to heating and melts the imperfect crystals. Many metals, in turn, melt sharply and reversibly as long as nuclei remain after melting for subsequent crystallization during the cooling cycle. Their analysis is complicated, however, due to thermal conductivity limitations of the calorimeters. Polymers of sufficiently high molar mass, finally, show a small amount of reversible, local melting that may be linked to partial melting of individual molecules. Experiments by temperature-modulated calorimetry and model calculations are presented. The samples measured included poly(ethylene terephthalate), poly(ethylene oxide)s, and indium. Two unsolved problems that arose from this research involve the origin of a high, seemingly stable, reversible heat capacity of polymers in the melting region, and a smoothing of melting and crystallization into a close-to-elliptical Lissajous figure in a heat-flow versus sample-temperature plot.

Keywords: Crystallization; Crystal nucleation; Irreversible melting; Locally reversible melting; Melting; Molecular nucleation; Temperature-modulated calorimetry

1. Introduction

For quantitative analysis of melting or crystallization with standard differential scanning calorimetry (DSC), one can identify four temperature regions of analysis. (1) The region of small changes in heat capacity before melting. This region is characterized by continued steady state, negligible temperature gradient within the sample, and a small, constant temperature gradient between sample and sample-temperature sensor. (2) The region of constant sample temperature where the transition is sharp and of sufficiently high heat of transition. On crystallization with supercooling of the sample, the heat of crystallization may raise the sample temperature to the melting temperature. If a constant-temperature region is reached, this second region is also close to steady state, but the sensor temperature may deviate more from the sample temperature due to the increase in heat flow. The amount of deviation depends on the

*Corresponding author. Tel.: +1-423-974-0652; fax: +1-423-974-3419.

[1] "The submitted manuscript has been authored by a contractor of the US Government under the contract No. DE-AC05-96OR22464. Accordingly, the US Government retains a non-exclusive, royalty-free license to publish, or reproduce the published form of this contribution, or allow others to do so, for US Government purposes."

[2] Present Address: Toray Industries, Inc., Otsu, Shiga 520, Japan.

[3] Present address: Toray Research Center, Inc. Otsu, Shiga 520, Japan.

0040-6031/98/$ – see front matter
PII: S0040-6031(98)00525-5

calorimeter construction and the control circuit governing the calorimeter. (3) This actual transition region 2 is followed by an approach to the new steady state that removes the larger difference between sample temperature and sensor. (4) The region of the melt or crystal when steady state similar to region 1 has been reached after the transition. The heat of transition absorbed or evolved over these four regions can be assessed by the baseline method [1].

In this paper, an analysis will be given of the analysis of melting and crystallization by temperature-modulated differential scanning calorimetry (TMDSC). In the first and fourth regions of the transition one can determine the 'reversing' heat capacity as the first harmonic of a Fourier series of the heat flow versus time; in the second and third, one must analyze the heat flow in the time-domain, i.e. plot the raw heat-flow signal HF(t) and correct for the sinusoidal heat-capacity baseline. If the transition covers more than one modulation cycle, the transition regions 1–4 overlap and complicate the quantitative analysis. If the transition is fully irreversible and not affected by the modulation, i.e. it has a rate practically constant over the temperature range $\pm A_T$, the reversing heat flow may be entirely due to the reversible heat capacity.

The TMDSC used in this research is modulated at the block temperature $T_b(t)$ with a sinusoidally changing amplitude which is governed, as in standard DSC, by adjusting the temperature of heater input at the sample position:

$$T_b(t) = T_0 + \langle q \rangle t + A_{T_b} \sin \omega t \quad (1)$$

where $\langle q \rangle$ is the underlying, constant heating rate and T_0, the initial isotherm at the beginning of the scanning experiment. The modulation amplitude at the block, A_{T_b} is adjusted by the control circuit so that the modulation amplitude of the sample sensor is A_T, as chosen by the operator. The modulation frequency ω is equal to $2\pi/p$ with p representing the duration of one cycle (in s). At steady state the sample is modulated with the same frequency, but with a phase lag of ε. Temperature-modulated calorimeters (TMC) constructed and/or controlled differently may deviate somewhat from the calorimetric responses described in this paper.

Measurements can be made as soon as steady state is reached, either under quasi-isothermal conditions ($\langle q \rangle = 0$) at T_0 [2], or with the linear temperature ramp $\langle q \rangle t$. The former method is equivalent to the classical AC calorimetry, the latter case corresponds to true temperature-modulated DSC. A detailed mathematical description [3] and a modeling scheme of the software used for data analysis [4] have been given. More extended discussions of the melting of poly(ethylene terephthalate) (PET) [5,6], poly(oxyethylene) (POE) [7,8] and indium (In) [9] discussed in this paper are available for further details and data on a larger number of samples. Work on paraffins and liquid crystals is in progress and will be submitted for publication in the near future.

2. Experimental details

A commercial Thermal Analyst 2920 MDSC system from TA Instruments was used for all measurements (modulated differential scanning calorimeter, MDSC™). Dry N_2 gas with a flow rate of 10–30 ml/min was purged through the sample. Cooling was accomplished by a mechanical refrigerator (RCS). For heat-flow-amplitude calibration ca. 25 mg of sapphire were used. The pan weights were ca. 23 mg and corrected for asymmetry [10]. The temperature calibration was carried out using the onsets of transition peaks for several standards. The PET was of industrial grade with a M_w of 18 000 Da with different thermal histories. The POEs had molar masses of 1500 and 4540 Da (POE1500, and POE5000, respectively). The In was of melting-point-standard grade. A modulation period, p, of 60 s was used at various amplitudes and underlying heating rates $\langle q \rangle$. The standard DSC was used with a heating rate of 10 K/min. Sample masses were chosen to maintain steady state for the regions of quantitative measurement of heat capacity (1–10 mg, depending on experiment design).

3. Results and discussion

3.1. Melting and crystallization rates

Fig. 1 shows a schematic diagram of the linear melting and crystallization rates of crystals of rigid, small monomer molecules and flexible, linear oligomers and polymers in the presence of crystal nuclei. This diagram is based on experiments on supercooling

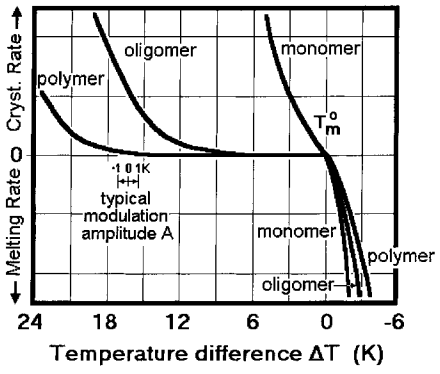

Fig. 1. Schematic of melting and crystallization rates of polymers, oligomers, and monomers. The rates are measured as rates of change of the linear crystal dimensions. (Typical polymer: poly(oxyethylene) of 35 000 Da, typical oligomer poly(oxyethylene) of <10 000 Da, typical monomer metals like In or Se_2).

and superheating, and comparisons of the kinetics of melting and crystallization over the last 100 years on materials like SiO_2, felspars, GeO_2, P_2O_5, Se_2, Se_x, POE, polyethylene, polyoxymethylene, polytetrafluoroethylene, polycaprolactam, and In (for Refs. see [5,11]). Obvious is the metastable range of temperature for the melt of flexible molecules which increases with molar mass and is characterized by negligible melting *and* crystallization rates, even in the presence of crystal nuclei. In this temperature region no polymer crystals can grow from the melt. The region of metastability is caused by the need of molecular nucleation for the crystallization of flexible molecules [11]. Modulation of the indicated magnitude cannot produce reversing melting/crystallization processes since the melting and crystallization regions can not be covered by the modulation amplitude of the temperature. When analyzing crystals on heating with $\langle q \rangle$ and a modulation of ± 1.0 K, melting will occur on the heating cycle when reaching temperature close to T_m^0, but at such temperatures *no* crystallization can occur on the cooling cycle. This leads to a very asymmetric response in TMDSC close to T_m^0 with a melting peak in one or more of the modulation cycles. A reversing contribution to the heat flow can be seen in this case, but is based on an erroneous assignment of the amplitude of the first harmonic similar to the reversible In melting, discussed below with the help of Fig. 4.

For monomers, as well as polymers, melting is often (but not always) so fast, to be limited only by thermal conductivity [11]. Both, DSC and TMDSC give under such conditions only limited information on the kinetics of melting, but can be used for measurement of the heat of fusion. The heat of fusion is separated from the heat-capacity effect by the well-known baseline method [12]. In TMDSC the total heat flow can be analyzed similarly, but may be less precise because of the lower heating rates commonly used in TMDSC. In sharp-melting substances, an analysis of the reversing signal in the time-domain is also possible, as described below.

Crystallization can be slowed sufficiently by experimenting close to the melting (high-temperature crystallization) or glass transition (cold crystallization). The crystallization is then measured by quick cooling or heating to the crystallization temperature and followed by isothermal measurement of the evolved heat.

With TMDSC new methods can be added to the analysis of crystallization. For example, one can gain kinetic information if the change of heat-capacity during crystallization is sufficiently large and reversible and the evolution of the latent heat is completely irreversible, as is expected for flexible molecules (see Fig. 1). Quasi-isothermal TMDSC can in this case separate the non-modulatable heat of transition from the reversible heat capacity and derive kinetic data from the changes in heat capacity with time which occurs during the phase transition. The lower limit of time for such experiment is about two modulation periods, and there is no limit to longer times since the heat capacity is continuously determined anew.

3.2. Melting of perfect polymer crystals

Fig. 2 shows DSC and quasi-isothermal TMDSC traces for a well-crystallized, low-molar-mass poly (oxyethylene), a flexible macromolecule [(O–CH_2–CH_2–)$_x$]. As expected from the schematic of Fig. 1, the well-crystallized POE5000 shows no crystallization, and accordingly, no renewed melting after the initial heating to T_0 [7]. To assure steady state in the evaluation of quasi-isothermal experiments, only data after the first 10 min ($10\times p$) are included in the analysis. Analysis of this sample by TMDSC with an underlying heating rate $\langle q \rangle$ by deconvolution of the reversing heat flow would not be possible because of loss of steady state, as will be described below. In the time-domain, one or more melting contribution would

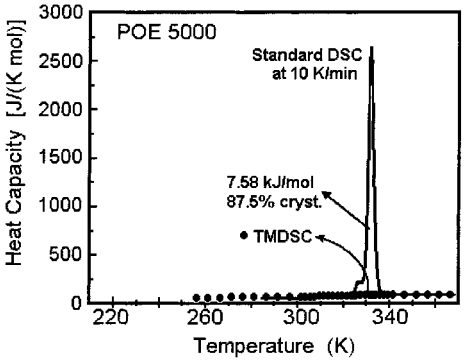

Fig. 2. Standard DSC and quasi-isothermal TMDSC of well-crystallized POE5000. Standard DSC at 10 K min; TMDSC at p=60 s, A_T=0.5 K, data collection during the last 10 min of a 20 min run.

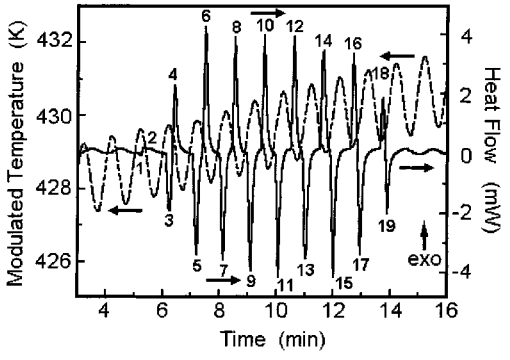

Fig. 3. Time-domain recording of the melting of In by TMDSC. Even numbers indicate crystallization peaks, odd ones, melting. Peaks 5–15 correspond closely to the heat of melting/crystallization (±28.6 J g^{-1}). Run parameters: p=60 s, A_T=1.0 K, mass of In, m=1.085 mg, $\langle q \rangle$=0.2 K min^{-1}.

occur in the high-temperature parts of the modulation cycles when traversing the melting region. The analysis of these time-dependent responses would require information about the heat conductivity of the calorimeter and change with $\langle q \rangle$.

The change from steady state before melting (1) into the new steady state in the sharp melting range with constant sample temperature (2) is handled easily by standard DSC (see Fig. 2). The return from the melting peak at the end of melting (3) to the baseline (4) is governed by the thermal conductivity of the calorimeter. The four different segments of the melting peak have been described using the linear Fourier differential equation describing thermal conductivity and lead to the common base-line analysis of the heat of fusion by DSC [12]. In TMDSC such abrupt changes in heat flow must similarly be analyzed in the time-domain, as will be shown next on the example of In. A deconvolution of the total heat flow from the reversing portion is not possible under the given conditions because of an overlap of the three regions of steady state and the approach to steady state, described above and in Section 1. Only if the heat-flow response to the modulation is close to sinusoidal does a deconvolution of the type used in TMDSC give quantitative information on a reversing heat flow or heat capacity.

3.3. Melting and crystallization of Indium

Fig. 3 illustrates the practically reversible melting of In, a sharp-melting metal, on traversing the melting temperature (429.75 K) with TMDSC in the presence of crystal nuclei [9]. Note the enormous increase in heat flow in the melting/crystallization range. The temperature modulation recorded by the sample thermocouple is affected much less, but regions of deviation exist during melting and crystallization. Still, the four regions of analysis overlap as shown by the time-domain plot. Analysis can be attempted with the baseline method. In TMDSC the baseline is the shallow, sinusoidal recording as it is seen before and after melting and crystallization. Fortunately crystalline and melted In have the same heat capacity, i.e. no adjustment of the base-line amplitude is needed.

Fig. 4 shows the analysis of a melting peak followed by crystallization within one modulation period using the modeling software of Ref. [4]. It shows that the reversing heat-flow amplitude, $\langle A_{HF} \rangle$, and its smoothed output show unrealistic features and are largely broadened. Both of them have no relation to the true amplitude of the heat of fusion or crystallization that was given as the input, HF(t). The analysis of the maximum amplitude makes no distinction between endotherm and exotherm, i.e. one could not distinguish between excess melting or crystallization. This figure shows clearly the limitations of the deconvolution software that makes use of the first harmonic only. All information must be extracted from the time-domain recording shown in Fig. 3.

With Fig. 5 a similar melting experiment with In is illustrated [9], but in the quasi-isothermal mode ($\langle q \rangle$=0) and with a much smaller modulation

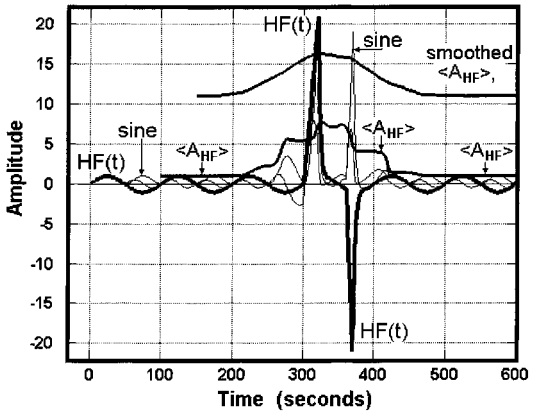

Fig. 4. Modeling of the pseudo-isothermal heat flow with a melting and crystallization peak using the Lotus 1–2–3™ software described in [4]. The final output, the smoothed $\langle A_{HF} \rangle$ is shifted by +10 amplitude units for clarity. The thin lines represent the Fourier components of the deconvolution.

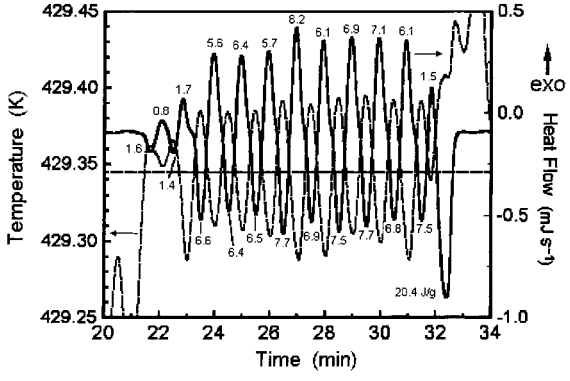

Fig. 5. Quasi-isothermal melting of In at 429.345 K. Run parameters: p=60 s, A_T=0.05 K, mass of In, m=1.085 mg, $\langle q \rangle$= 0.0 K min^{-1}. The numbers next to the transition peaks give the approximate heat of transition.

amplitude (±0.05 K). Before 22 min, one can see the end of the previous experiment at T_0=429.245 K, and after 32 min, the beginning of the experiment at T_0=426.445 K. Both, the earlier and later recordings show no trace of melting or crystallization and have the normal, low-amplitude, sinusoidal heat flow due to heat capacity only. In the melting region (T_0= 429.345±0.05 K) clearly the time for melting is insufficient to supply all heat of fusion, only ca. 1/3 of the In melts. Such quasi-isothermal experiments can be used for calibration of the calorimeter. In the present case a correction of +0.4 K must be applied to the data. A detailed inspection of the melting and crystallization peaks shows practically no supercooling. Since melting is never complete, there is always a steep reversal of the melting endotherm to the crystallization exotherm as soon as the temperature of the sample reverses. Note that despite constant temperature of large parts of the sample, the sample-sensor is continuously modulated with only minor deviation from the sinusoidal change. Much can be learned about the loss and partial attainment of steady state from these graphs. The small crystallization peak in Fig. 5 at 23 min, for example, shows clearly the first part of an approach to steady state after complete crystallization as can be seen better for the large-amplitude modulation of Fig. 3. To reach repeatability of the quasi-isothermal melting and crystallization is seen to take somewhat more than 2 min. With the limits of fully irreversible and close to reversible melting established in Sections 3.2 and 3.3, intermediate cases can be treated next.

3.4. Locally reversible melting of polymers

Figs. 6 and 7 display an initial study of the melting and crystallization of melt-crystallized and melt-quenched poly(ethylene terephthalate) (PET) [(O–CH_2–CH_2–O–CO–C_6H_4–CO–)$_x$]. The data were generated with standard DSC and quasi-isothermal TMDSC for Fig. 6 and quasi-isothermal TMDSC only, for Fig. 7 [5]. The reversing component in the melting region of the TMDSC traces was quite sur-

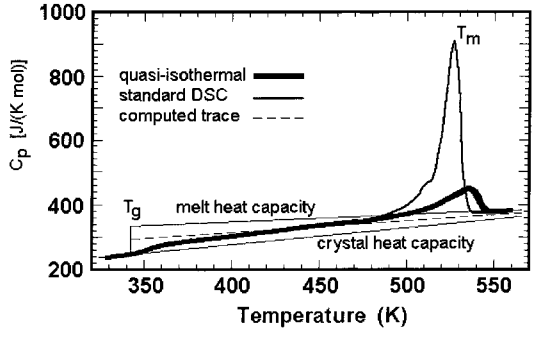

Fig. 6. Reversible melting of poly(ethylene terephthalate). Melt-crystallized sample of 44% crystallinity. Standard DSC 10 K min^{-1}. TMDSC run parameters: p=60 s, A_T=1.0 K, mass of PET, m=5.00 mg, $\langle q \rangle$=0.0 K min^{-1}. Recorded data are the last 10 min of a 20 min experiment.

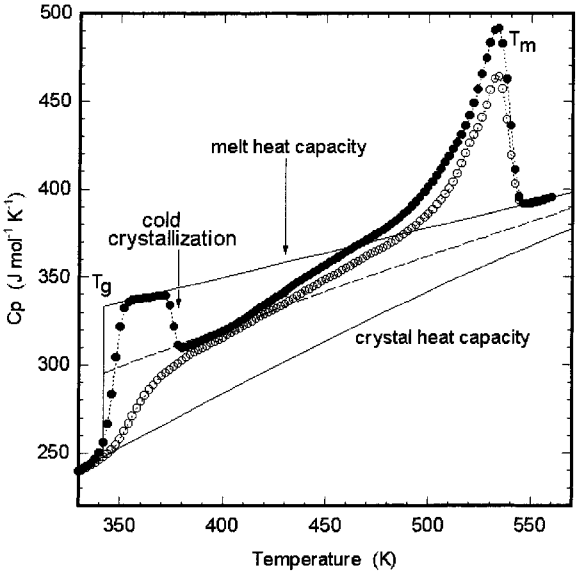

Fig. 7. Reversible melting of poly(ethylene terephthalate). Melt-quenched, amorphous sample (filled circles). TMDSC run parameters: p=60 s, A_T=1.0 K, mass of PET, m=5.00 mg, $\langle q \rangle$= 0.0 K min^{-1}. For comparison the quasi-isothermal data for the 44% crystalline sample are shown as open circles (note the difference in scale). Recorded data are the last 10 min of a 20 min experiment.

prising, since one would have expected from Fig. 1 that there is not latent heat contribution to the reversing signal, as was also demonstrated with Fig. 2. In the meantime, similar small endothermic responses to modulation in the melting region have been found in several other polymers, like high molar mass poly(oxyethlene) [7], poly(trimethylene terephthalate) [13], and poly(ether ether ketone) (PEEK) [14]. This observation seems, thus, generally true for high-molar-mass polymers.

Fig. 7 reveals that the contribution to the apparent reversing heat capacity from melting and crystallization is dependent on the degree of perfection of the crystals. The poorer melt-quenched crystals have a higher reversing 'melting peak'. This reversing melting can thus be used to characterize a polymeric material. Poorer crystallized molecules have higher reversing melting contributions and perfect crystals show none. The origin of this reversing melting was linked to a small amount of melted polymer that could not be extracted with solvents [5]. It fits also into the general concept of molecular nucleation as the cause of the metastable region between melting and crystallization in Fig. 1 [11]. One assumes that at the moment of stoppage of melting due to the decrease in temperature at the appropriate modulation phase, a small number of molecules remain partially crystallized, i.e. they do not have to undergo renewed molecular nucleation for crystallization. This permits these partially melted molecules to be close to (locally) reversible, i.e. recrystallize during the cooling cycle and remelt during the next heating cycle.

The cold-crystallization region in Fig. 7 illustrated the possible measurement of crystallization kinetics mentioned in Section 3.1. by following the decrease in heat capacity on going from the supercooled melt to the crystalline state as described in Section 3.1. Because of the large degree of supercooling, the evolution of the heat of crystallization is irreversible and does not change in rate over the modulation amplitude. In this case all heat of crystallization appears in the total heat flow and only the reversible heat capacity is recorded as the reversing heat capacity.

Fig. 8 shows that the apparent, reversing heat capacity in the melting region grows smaller with time [6]. After 6 h at the marked temperature, the level of the liquid heat capacity is reached. Even when extrapolating to infinite time, using an exponential fit of the changing reversing heat capacity, the sample does not reach the semicrystalline heat capacity level, but only

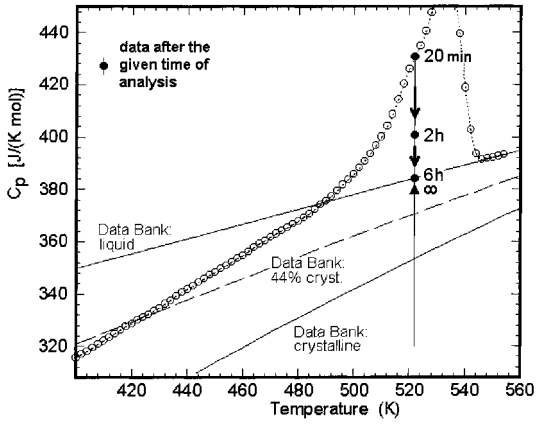

Fig. 8. Change of reversible melting of poly(ethylene terephthalate) with time. Melt-crystallized sample of 44% crystallinity and conditions as in Fig. 6. The measurement at the indicated filled circle was extended from 20 min to 6 h and then extrapolated to infinity.

the point marked by the filled triangle. These long-time experiments show that the local structures that give rise to the extra reversing heat capacity contribution are not stable, but disappear in time. It is interesting to note that this disappearance may have two opposite reasons. First, the molecules that show the locally reversible melting may perfect in time and thus their melting temperature will fall outside the modulation limit. Second, their melting may, in time, progress to a sufficiently large degree so that an insufficient attachment to the crystal exists to overcome the nucleation barrier. In this case, the subsequent supercooling in the low-temperature cycle is insufficient to cause crystallization. Further experiments with different temperature-modulation periods and amplitudes may give additional information if one or both of the proposed mechanisms are active and permit considerable progress in the understanding and analysis of the defect structure of polymer crystals.

The higher-than-expected heat capacity after long-time experiments has not found an explanation as yet. It also seems a general observation in high-molar-mass polymers and may go beyond the heat-capacity contribution due to the introduction of thermal point-defects, as documented with *gauche* defects in glassy and crystalline polyethylene [15].

3.5. Reversible melting of defect polymer crystals of low molar mass

Fig. 9 illustrates another case of apparent, reversible melting and crystallization [7]. Standard DSC and quasi-isothermal TMDSC data are shown for a melt-quenched, poorly crystallized POE of low molar mass (oligomer). The small reversing heat-capacity contribution is this time at the low-temperature side of the melting peak and can be made to disappear by more careful crystallization before melting, as shown for the higher molar mass sample of Fig. 2. The interpretation of the data points to a small amount of poorly crystallised POE of even lower than the 1500 Da of the main portion of the sample [8].

Fig. 10 shows the Lissajous figure of a plot of heat flow HF(t) versus the modulated sample temperature $T_s(t)$. If both quantities are sinusoidal at the same frequency, elliptical Lissajous figures should arise. The POE 1500 has, however, some distortions due to a small amount of melting and crystallization. The

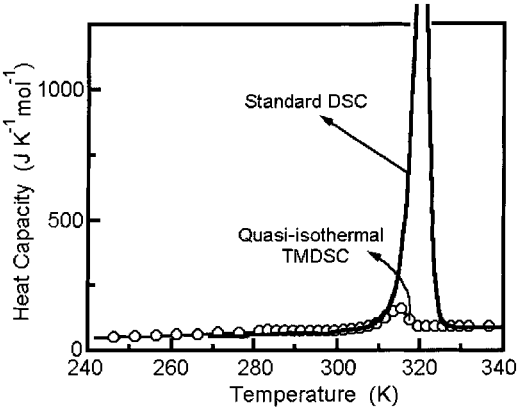

Fig. 9. Standard DSC and quasi-isothermal TMDSC of quickly cooled POE1500. Standard DSC at 10 K/min; TMDSC at p=60 s, A_T=0.5 K, data collection during the last 10 min of a 20 min run.

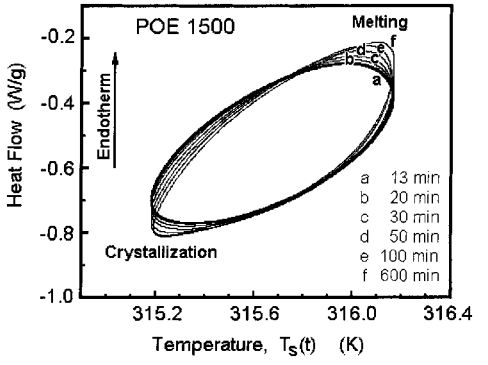

Fig. 10. Lissajous figures of the sample of Fig. 9 as a function of time at 315.7 K; TMDSC at p=60 s, A_T=0.5 K, data collection at the time indicated in the figure, mass of POE, m=1.00 mg, $\langle q \rangle$=0.0 K min^{-1}.

positions of the distortions indicate that there is a metastable region between the oligomer melting and crystallization. In contrast to the high-molar-mass reversing melting, Fig. 10 shows that in this case the heat-flow amplitude increases with analysis time, rather then decreases. It was suggested [8] that diffusion of the proper species of the crystallization sites may cause the slow increase. It is not fully resolved why the indication of melting and crystallization in the Lissajous figures are not more obvious. A frequent observation is that in the early figures, before reaching steady state much clearer deviations occur from the

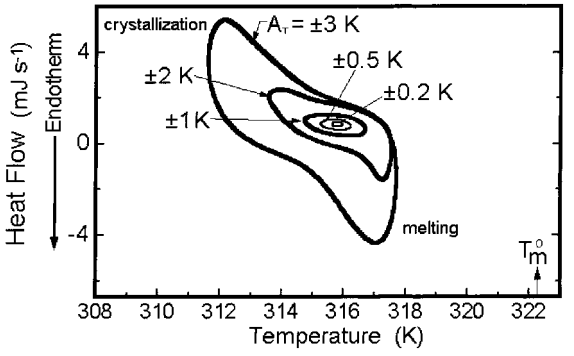

Fig. 11. Lissajous figures of the sample of Fig. 9 as a function of modulation amplitude at 315.76; TMDSC at p=60 s, A_T as indicated in the figure, data collection during the last 10 min of a 20 min run.

ellipse. In time, an ellipse is approached, but the heat-flow amplitude is not decreased.

Fig. 11 illustrates the change in the Lissajous figures for a sample as in Fig. 10 for different modulation amplitudes A_T. By increasing A_T beyond 0.5 K for the chosen temperature, increasing melting and crystallization can be seen distorting the ellipse. The positions of the melting and crystallization during the modulation pointing to the growth of metastable crystals with a lower melting temperature. Fig. 12 indicates the magnitude of shift that has been accomplished relative to the melting temperatures of the perfect crystal. The melting curve in Fig. 12 was chosen to match the observed data with the known growth rates [8]. The region of metastability of the

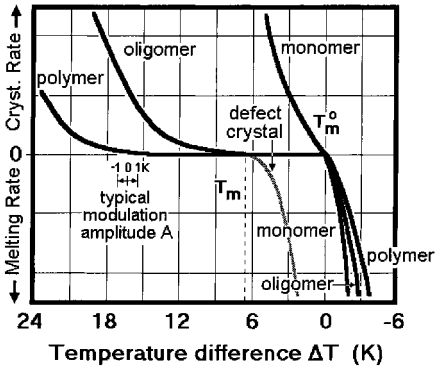

Fig. 12. Schematic lowering of the melting rate of a poor oligomer crystal to explain the observation of some reversing melting (compare to Fig. 1).

melt has been narrowed because the crystals that grow under the given conditions are poor and do not have sufficient time to perfect before melting. As in the case of In melting, the distortion of the sinusoidal response to temperature modulation invalidates equating of the reversing heat capacity to the first harmonic of the Fourier analysis, but quantitative data can be gained in the time-domain. The use of TMDSC has in this case an application for the discovery of low molar mass, crystallizable impurities in the sample. Furthermore, TMDSC with different modulation amplitude and frequency can be used to probe the melting/crystallization diagram of Figs. 1 and 12. It is useful for the study of Figs. 1 and 12 to be able to extend the amplitude to as high as ±10 K with an appropriately chosen low modulation frequency (>100 s).

4. Conclusions

This work has shown, just as the analysis of the glass transition presented at last year's ICTAC meeting [16], that TMDSC can produce important new and different quantitative information relative to standard DSC. It makes it particularly clear that for some analyses standard DSC is faster and/or more suitable, but for others, only TMDSC can give sufficient information by using one or more of its various measurement and analysis methods. In TMDSC as well as DSC, care must be taken that the basic conditions for quantitative measurements and data analyses are known and satisfied [1]. In particular, one cannot use instrumentation or software that is not fully described or disclosed by the manufacturer.

A fully equipped thermal analysis laboratory should have DSC as well as TMDSC available, and a decision must be made for every sample whether one, the other, or both methods are needed for best and quickest results [17]. Most efficient seems a fast DSC trace at 10–20 K min^{-1}. On inspection of this trace, further decisions can be made about introduction of various thermal or mechanical histories and regions of interest for slow TMDSC (often <1.0 K min^{-1}) or quasi-isothermal TMDSC at selected temperatures.

The basic diagram of melting/crystallization could be verified and the limits of TMDSC were established by comparing the melting of a broad range of materials using time-domain and Fourier transforms to heat-

flow amplitudes. Direct observation of partial melting of polymer molecules is possible and gives information about the crystal–melt interface. Low-molar-mass crystals of poor crystal perfection could be seen in the presence of a large volume of more perfect crystals. Both of these analyses can give new information about crystal and molecular morphology, not available before. A number of unexplained observations involve seemingly high reversible heat capacities in the melting region and smoothing of the Lissajous figures on long-time modulation in the presence of phase transitions.

Acknowledgements

This work was supported by the Division of Materials Research, National Science Foundation, Polymers Program, Grant # DMR-9703692 and the Division of Materials Sciences, Office of Basic Energy Sciences, U.S. Department of Energy at Oak Ridge National Laboratory, managed by Lockheed Martin Energy Research Corp. for the U.S. Department of Energy, under contract number DE-AC05-96OR22464. Support for instrumentation came from TA Instruments, Inc. and Mattler-Toledo Inc. Research support was also given by ICI Paints

References

[1] B. Wunderlich, in: E. Turi (Ed.), Thermal Characterization of Polymeric Materials, Academic Press, San Diego, 1997.
[2] A. Boller, Y. Jin, B. Wunderlich, J. Thermal Analysis 42 (1994) 307.
[3] B. Wunderlich, Y. Jin, A. Boller, Thermochim. Acta 238 (1994) 277.
[4] B. Wunderlich, J. Thermal Analysis 48 (1997) 207.
[5] I. Okazaki, B. Wunderlich, Macromolecules 30 (1997) 1758.
[6] I. Okazaki, B. Wunderlich, Macromol. Chem. Phys., Rapid Commun. 18 (1997) 313.
[7] K. Okazaki, B. Wunderlich, Macromolecules 30 (1997) 4126.
[8] K. Ishikiriyama, B. Wunderlich, J. Polymer Sci., Part B, Polymer Phys. 35 (1997) 1977.
[9] K. Ishikiriyama, A. Boller, B. Wunderlich, J. Thermal Analysis, 50 (1997).
[10] A. Boller, I. Okazaki, K. Ishikiriyama, G. Zhang, B. Wunderlich, J. Thermal Analysis 49 (1997) 1081.
[11] B. Wunderlich, Macromolecular Physics, Vol. III, Crystal Melting, Academic Press, New York, 1980.
[12] B. Wunderlich, Thermal Analysis, Academic Press, Boston, 1990.
[13] M. Pyda, A. Boller, J. Grebowicz, H. Chuah, B. Wunderlich, Thermochim. Acta, this issue.
[14] C. Schick, private communication.
[15] B. Wunderlich, Thermochim. Acta 300 (1997) 43.
[16] B. Wunderlich, I. Okazaki, J. Thermal Analysis 49 (1997) 57.
[17] B. Wunderlich, J. Thermal Analysis 49 (1997) 7.